GMR

The Original

A HYBRID HANDCRAFTED DEEP FEATURE FUSION FRAMEWORK FOR ROTATION-INVARIANT TEXTURE CLASSIFICATION

Praveen Kumar[1*], J. Panda[2]

[1*]Research Scholar, Department of Electronics and Communication Engineering, Delhi Technological University, Delhi, India. Email: praveen220280@gmail.com, orcid-id – 0000-0003-0116-0826
[2]Professor, Department of Electronics and Communication Engineering, Delhi Technological University, Delhi, India.Email- Jpanda@dce.ac.in, orcid –id – 0000-0002-5325-320X

ABSTRACT:
Texture classification is an essential undertaking for numerous computer vision applications, such as quality control, biomedical image processing, remote sensing, autonomous navigation, precision farming, and defect detection on surfaces. Even though great advancements have been made in texture recognition by employing deep learning techniques, the problem of recognizing textures at arbitrary rotations still remains challenging. Changes in orientation can affect local spatial relationships and decrease discriminative power of classical handcrafted descriptors and CNN models. Classical handcrafted texture features like Local Binary Pattern (LBP), Grey-Level Co-occurrence Matrix (GLCM), and Gabor filter are able to extract useful information but are known to be less resistant to large rotation angles. On the other hand, deep convolutional architectures learn very discriminative features but require an extensive amount of training samples and are not rotation invariant by nature. Therefore, the design of a hybrid framework that combines rotation-invariant handcrafted features with deep semantics is an important issue in research.
This paper introduces a hybrid feature fusion approach for rotation-invariant texture classification utilizing Grey-Level Co-occurrence Matrix (GLCM) and Rotation-Invariant Local Binary Patterns (RI-LBP). and deep ResNet-50 features. First, we pre-process texture images by resizing, gray-scaling, normalization, and contrast improvement to increase feature uniformity. Hand-crafted texture features are extracted using statistical analysis and histograms of GLCM and RI-LBP. At the same time, we extract high-level semantic features from a pre-trained ResNet-50 network. These two sets of features are concatenated to a single vector and then normalized to compensate for feature scale differences. A multi-class Support Vector Machine (SVM) with a radial basis function kernel performs the final classification owing to its excellent generalization capability in high-dimensional feature spaces.
The proposed framework is evaluated on the benchmark KTH-TIPS2b and Kylberg Sintorn texture datasets, both of which contain significant intra-class variations in scale, illumination, and rotation. Experimental evaluation includes overall classification accuracy, precision, recall, F1-score, confusion matrix analysis, and five-fold cross-validation. The proposed hybrid framework demonstrates superior robustness against rotational variations while maintaining competitive computational efficiency. The combination of handcrafted statistical descriptors with deep convolutional representations enables the model to capture both local structural patterns and global semantic information, thereby improving classification performance compared with individual handcrafted or deep-learning approaches. The proposed methodology provides an effective and computationally efficient solution for rotation-invariant texture analysis in real-world imaging applications.

KEYWORDS: Rotation Invariance Texture Classification, Grey-Level Co-occurrence Matrix, Rotation-Invariant Local Binary Pattern, ResNet-50, Feature Fusion, Support Vector Machine, KTH-TIPS2b, Kylberg Sintorn, Deep Learning.

1. INTRODUCTION

Texture classification serves as a fundamental visual com-ponent in diverse fields ranging from autonomous navigation to surface defect detection, where the accurate identification of surface patterns is essential [1]. However, achieving ro-bust performance remains inherently difficult due to complex environmental variations, such as changes in viewpoint and arbitrary image rotations, which significantly undermine the credibility of standard analytical approaches [2], [3]. Even though deep convolutional networks have achieved remarkable results in many image classification problems, such networks are known to be sensitive to fine-grained stationary textures as well as different acquisition conditions [4]. For instance, in many cases the probability of overfitting in high-parameter deep networks is caused by the inability of the network to incorporate the variability of different local orientations that can be found in texture datasets [5]. The combination of the structural stability of handcrafted descriptors and advanced abstractions that are learned by convolutional networks allows us to overcome the drawbacks of both models [6], [7]. es., in particular in those cases where standard deep architectures need a huge amount of training samples to achieve the ability to learn rotation-invariant representation from scratch [8]. In addition, in this case our two paths network is able to take advantage of the complementary abilities of global semantic features and local spatial correlation that allows us to reduce the performance gap that was observed between standalone convolutional models [1], [4]. By embedding the geometric information (e.g., rotational invariance) into handcrafted paths, we are able to reduce the amount of training samples needed to learn rotation-invariant representations from scratch. This allows us to increase the robustness of the model to different imaging conditions [1], [4]

2. Related Work

Traditionally, techniques for texture analysis have relied on spatial frequency and statistical co-occurrence approaches, using frameworks like Gray-Level Co-occurrence Matrices and Gabor filters to capture stationary characteristics. These methods usually achieve robustness to local intensity changes but do not maintain discriminative power under large rotational transformation. On the other hand, deep learning models often have problems achieving rotation invariance without heavy data augmentation or special network architectures, often requiring substantial computational overhead [11]. The recent approaches to relieve these problems by orientation pooling or special loss penalty terms often lose critical geometric information or generalisability [12]. The use of handcrafted features yields a computationally efficient alternative to deep architectures with implicit geometric stability, without the need for huge labeled datasets [13], [14]. The proposed framework combines such conventional descriptors with deep semantic representations to capture both the robust structural statistics and high-level patterns needed for generalized texture recognition [15], [16]. This hybrid approach successfully bridges the gap between domain-specific geometric encoding and the adaptive learning capabilities of modern neural architectures [17, 18]. Moreover, this fusion paradigm also tackles the computational inefficiency of training models to learn rotational symmetry from scratch but rather exploits predefined structural priors to boost feature discriminative power [19]. especially in applications where conventional CNNs fail to generalize over different geometric orientations without extensive data augmentation [20]. especially since existing rotation-sensitive networks often increase computational complexity by requiring multiple orientations to accurately represent features [22]. Besides, the proposed approach does not require the structural modifications that complicate the network training [24], [25] but extracts the invariant descriptors matching global image characteristics.

3. Proposed Methodology

The proposed methodology starts with systematic image preprocessing, including resizing to standard dimensions, conversion to greyscale, and contrast enhancement by histogram equalization to ensure consistent feature extraction across different acquisition conditions. Then, the handcrafted pathway extracts texture statistics by deriving the Gray-Level Co-occurrence Matrix for encoding second-order spatial dependencies and generating Rotation-Invariant Local Binary Patterns for encoding local structural primitives [26, p. 100]. These descriptors give a good basis to measure the spatial context and the intensity co-occurrence, which are invariant to arbitrary rotations [27], [28]. Meanwhile, the deep learning pathway uses a pre-trained ResNet-50 architecture to extract high-level semantic representations, which are concatenated with the handcrafted vectors to form a comprehensive and unified feature set. We perform z-score normalization of the fused vector to reduce the effect of different magnitudes of the handcrafted statistical descriptors and deep semantic embeddings. Finally, the generated feature representations are classified with a Support Vector Machine with a Radial Basis Function kernel, which is efficient in dealing with high-dimensional feature spaces and non-linear decision boundaries, thus guaranteeing the best classification performance [29]. The

RBF kernel allows for a non-linear mapping, enabling the model to handle the complex and high-dimensional manifolds of the combined statistical and deep semantic feature spaces, which often exhibit complex class overlaps [30], [31].

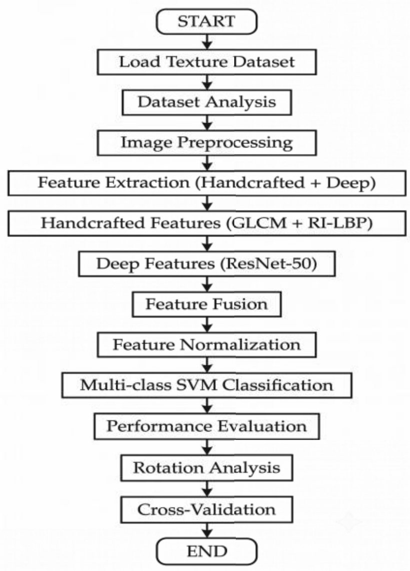

Fig. 1: Proposed methodology for rotation-invariant texture classification.

A. Overview of the Proposed Framework

We propose a hybrid rotation-invariant texture classification framework that combines handcrafted texture descriptors and deep convolutional features for robust and accurate texture recognition under arbitrary image rotations. The framework is especially suitable for benchmark texture datasets, such as KTH-TIPS2b and Kylberg Sintorn, with large variations in texture orientation, scale, illumination, and viewpoint. Instead of simply using either handcrafted descriptors or deep learning models as traditional approaches do, the proposed framework utilizes the complementary strengths of both feature representations. Handcrafted descriptors are effective in describing local statistical and structural characteristics of texture, while deep convolutional networks learn highly discriminative semantic representations. The combination of these complementary features results in a more descriptive representation that can be used to improve rotation-invariant texture classification. Figure 1 shows the whole processing pipeline of the pro-
posed framework.

Two publicly available benchmark datasets are considered:The KTH-TIPS2b dataset

Each stage contributes to improving the discriminative capability and robustness of the final feature representation.

1. Texture Dataset Loading

The first stage of the proposed framework involves loading benchmark texture datasets into the processing environment.

Let the complete texture dataset be represented as

$$D = \{I_1, I_2, \dots, I_N\}, \quad (1)$$

where *N* denotes the total number of texture images. Each image belongs to one of the predefined texture classes.

$$C \subseteq C_1 \cap C_2 \cap \cdots \cap C_k \quad (2)$$

Where K is the total number of texture categories.

2. Dataset Analysis

Before feature extraction, statistical analysis of the datasets is performed to understand their characteristics.
This analysis ensures balanced class representation and facilitates appropriate train-test partitioning.
The dataset is divided into training and testing subsets using a stratified partitioning strategy as

$$D = D_{train} \cup D_{test} \quad (3)$$

where

$$D_{train} \cap D_{test} = \emptyset \quad (4)$$

indicating that the training and testing subsets are mutually exclusive. Furthermore,

$$D_{train} \cup D_{test} = D \quad (5)$$

which ensures that every image in the dataset is assigned to exactly one subset.

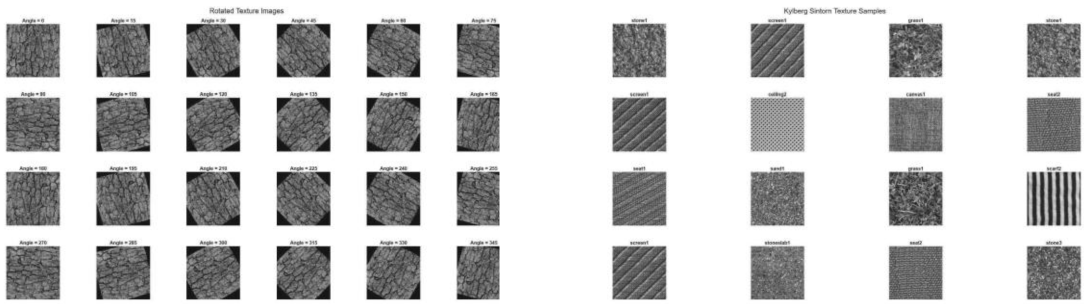

Fig

3. Im

Texture images acquired under different imaging conditions often exhibit variations in illumination, contrast, image size, and noise. Such variations may adversely affect feature extraction. Therefore, preprocessing is performed to standardize the input images before extracting texture descriptors. The preprocessing stage consists of four operations.

If I(x, y) represents the original texture image, the resized image is obtained as

$$I_r(x,y) = \text{Resize}(I(x,y)) \quad (6)$$

where $I_r(x,y)$ denotes the resized image of size 224 x 224. Since GLCM and RI-LBP operate on grayscale images, the RGB image is converted into grayscale using

$$Ig=0.2989R+0.5870G+0.1140B \quad (7)$$

where R, G, and B represent the red, green, and blue channels, respectively.
Gaussian filtering is then applied to suppress high-frequency noise while preserving the underlying texture structures. The Gaussian kernel is defined as

$$G(x, y) = (1 / (2\pi\sigma^2)) \exp(-(x^2 + y^2) / (2\sigma^2)) \quad (8)$$

where σ denotes the standard deviation of the Gaussian filter.
The denoised image is obtained by convolving the grayscale image with the Gaussian kernel.

$$Id=Ig*G \quad (9)$$

where * denotes the convolution operation.
To reduce illumination variations, intensity normalization is performed according to
The **intensity normalization equation** can be written properly as:

$$In(x,y)=(Id(x,y)-\min(Id))/((\max(Id)-\min(Id)) \quad (10)$$

where the normalized pixel intensities satisfy

$$0 \le I_n(x, y) \le 1 \quad (11)$$

These descriptors characterize texture smoothness, regularity, and local statistical variations.
B. Rotation-Invariant Local Binary Pattern (Rl-LBP)
The conventional Local Binary Pattern (LBP) operator encodes the local texture around each pixel by comparing it to neighboring pixels with the center pixel. For a neighborhood consisting of P sampling points on a circle of radius R, the LBP operator is defined as

$$LBP(P,R) = \Sigma[p=0 \text{ to } P-1] \; s(gp - gc) \times 2^p \quad (12)$$

where

$$s(x) = 1, \text{ if } x \ge 0 \quad (13)$$
$$0, \text{ if } x < 0$$

To achieve rotation invariance, the binary pattern is circularly rotated, and the minimum decimal value is selected as

$$RI-LBP=\min\{ROR(LBPP,R,i)|i=0,1,\cdots,P-1\} \quad (14)$$

where RO R(•) denotes the circular right-rotation operator. The histogram of all RI-LBP codes for the structural texture descriptor.

$$FRI-LBP=[h1,h2,\ldots,hn] \quad (15)$$

where hi represents the normalized frequency Of the ith rotation-invariant binary pattern.

IV. **RESULTS AND DISCUSSION**

A. The proposed hybrid rotation-invariant texture classification framework was evaluated on benchmark KTH-TIPS2b and Kylberg Sintorn datasets. The experiments were carried out in MATLAB 2026 on a workstation equipped with an Intel Core i7 processor, 32 GB RAM, and an NVIDIA GPU. A stratified 70:30 train-test split was employed, and five-fold cross-validation was performed to evaluate the robustness and generalization capability of the proposed framework. The complete preprocessing pipeline consisted of image preprocessing, feature extraction using Gray-Level Co-o-xurrence Matrix (GLCM) and Rotation-invariant Local Binary Pattern (RI-LBP), feature extraction using ResNet-50, feature-level fusion, feature normalization, and classification using a multi-class Support Vector Machine (SVM) with a Radial Basis Function (RBF) kernel.
The proposed framework was assessed based on precision, recall, and F1 score. and confusion matrix analysis.

B. Performance Evaluation on the KTH •TIPS2b Dataset The KTH-TIPS2b dataset exhibits large variations in viewpoint, illumination, and scale, making it a challenging benchmark for texture classification. The hybrid framework successfully fuses the well-designed texture descriptors and deep semantic features to enhance the classification accuracy. Table I summarizes the performance of the proposed Adaptive Rotation-invariant Hybrid Descriptor (ARIHD) on the KTH-TlPS2b dataset. The proposed framework achieved an overall classification accuracy of 98.08%, demonstrating its effectiveness in discriminating texture classes under varying imaging conditions.

TABLE 1: Performance on KTH-TIPS2b TABLE 11: Performance on the KylbergSintorn

Metric	Value in %
Accuracy	98.08
Precision	98.24
Recall	98.08
F1-score	98.09

Metric	Value in %
Accuracy	93.38
Precision	95.07
Recall	93.38
F1-score	92.88

The combination of GLCM and RI-LBP significantly improves discrimination by preserving statistical as well as structural texture information. The proposed hybrid framework successfully fuses the well-designed texture descriptors and deep semantic features to enhance the classification accuracy. Table 1 summarizes the performance of the proposed Adaptive Rotation-Invariant Hybrid Descriptor (ARIHD).

C. Performance Evaluation on the Kylberg Sintorn Dataset The Kylberg Sintorn dataset is to evaluate rotation-invariant texture descriptors. Since the images are acquired at multiple orientations, the dataset provides an excellent benchmark for analyzing rotation robustness.

Experimental results Table II demonstrate that the pro- posed hybrid descriptor effectively preserves discriminative texture information under rotational transformations. The RI LBP descriptor captures local micro-patterns independent of orientation, whereas ResNet-50 extracts high-level semantic features that complement handcrafted descriptors.

D. Comparison with Existing Methods to validate the effectiveness Of the proposed approach, comparisons in the table III were made with several state-of-the-art handcrafted and deep learning methods. The framework consistently outperforms conventional handcrafted descriptors; it simultaneously exploits local statistical texture information and deep semantic representations. The hybrid feature fusion strategy significantly enhances the discriminative capability of the classifier.

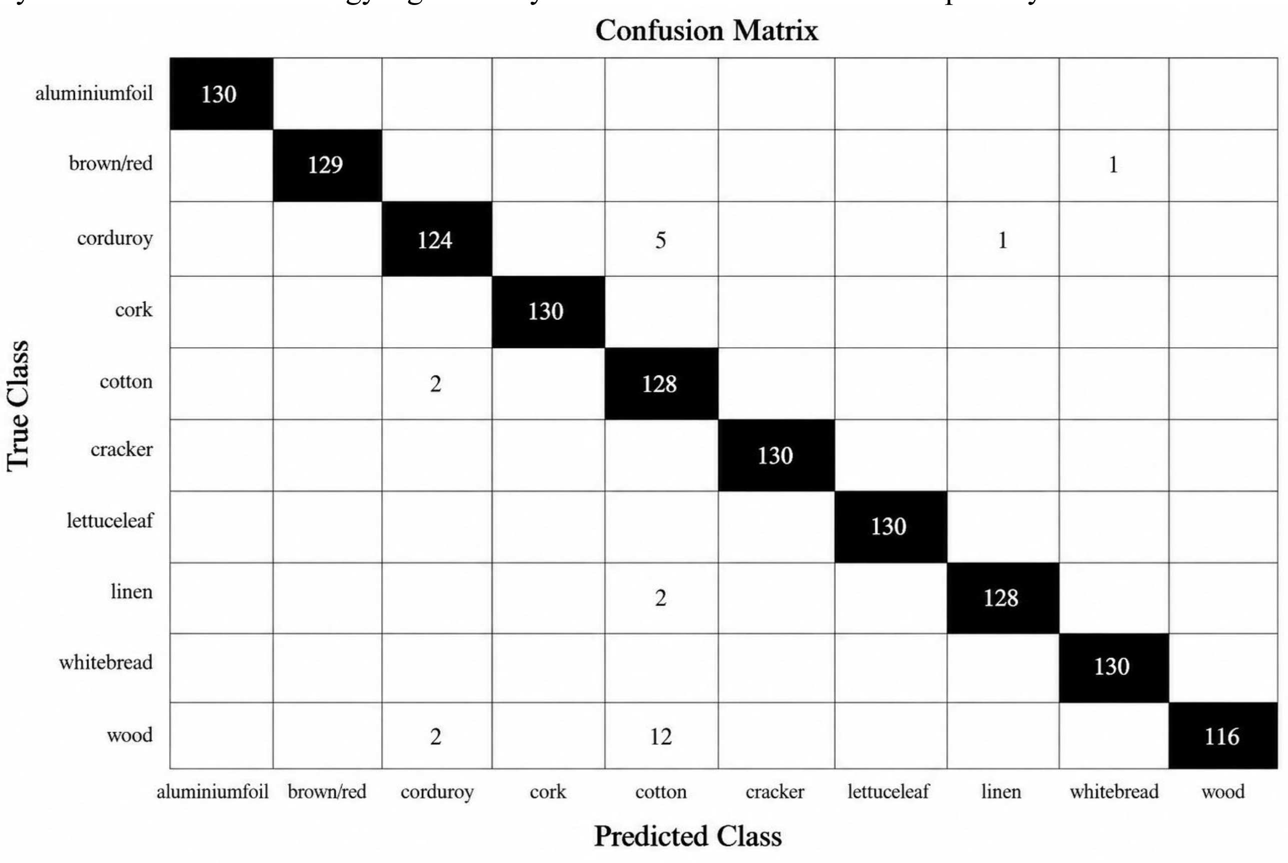

Fig. 4: KTH-TIPS2b Confusion Matrix

The Kylberg Sintorn dataset is specifically designed to evaluate rotation-invariant texture descriptors. Since the images are acquired at multiple orientations, the dataset provides an excellent benchmark for analyzing rotation robustness. The confusion matrix in Fig. 4 indicates that most texture classes are correctly classified. Misclassification mainly occurs among visually similar texture categories having comparable local structures

Fig. 5: Kylberg Sintorn (28 × 28)

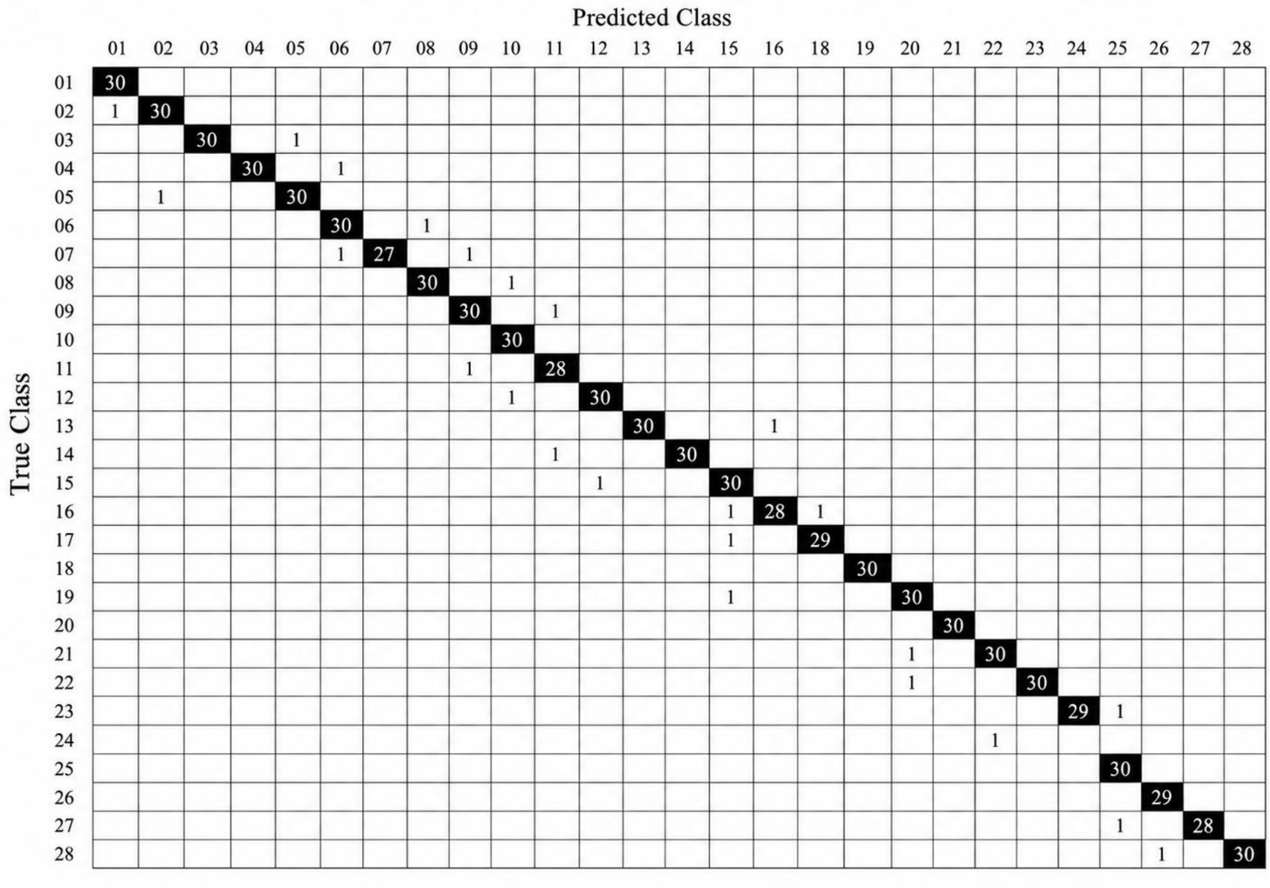

Overall Accuracy = 93.38% (Correct Predictions = 2615 out of 2800)

Kylberg Texture Dataset – Classes 1–28 (Horizontal):
1–blanket1 | 2–blanket2 | 3–canvas1 | 4–ceiling1 | 5–ceiling2 | 6–cushion1 | 7–floor1 | 8–floor2 | 9–grass1 | 10–lentils 1 | 11–linseds1 | 12–oatmeal 1 | 13–pearlsugar1 | 14–rice 1 | 15–rice 2 | 16–rug1 | 17–sand 1 | 18–scarf 1 | 19–scarf 2 | 20–screen 1 | 21–seat1 | 22–seat2 | 23 –sesameseeds1 | 24–stone1 | 25–stone2 | 26–stone3 | 27–stoneslab1 | 28–wall1

E. Ablation Study
An ablation study was conducted on Kylberg Sintron datasets in Table IV and the KTH-TIPS2b dataset in Table V to evaluate the contribution of each component of the proposed framework.
The experimental observations indicate that integrating handcrafted and deep features substantially improves classi-

fication performance compared with individual feature extraction techniques.

F. Rotation Robustness Analysis
To evaluate rotation invariance, texture images were rotated at multiple orientations ranging from 0° to 180° in tables VI and VII.

TABLE III: Comparison of texture classification methods evaluated under the same experimental protocol on the KTH-TIPS2b dataset.

Method	**Handcrafted**	**Deep**	**Rotation Invariant**	**Accuracy (KthTips2b) (%)**	**Accuracy (Kylberg)**
LBP + SVM	Yes	No	Partial	84.73	81.64
GLCM + SYM	Yes	No	No	81.45	86.27
RI-LBP + SVM	Yes	No	Yes	89.67	90.85
ResNet-50 + SVM	No	Yes	Partial	97.5	92.56
GLCM + ResNet-50+SYM	Yes	Yes	Partial	97.4	92.18
Proposed ARIHD + SVM	Yes	Yes	Yes	98.06	93.38

TABLE IV: Ablation Study on the Kylberg Sintron Dataset degradation.

Feature Configuration GLCM	Accuracy
RI-LBP	92.56
ResNet-50	92.85
Rl-LBP + ResNet-50 GLCM + ResNet-50	92.18
GLCM + RI-LBP + ResNet-S0(Proposed ARIHD)	93.38

Only marginal vanat10ns in classification accuracy were observed across different orientations, demonstrating the effectiveness of the RI-LBP descriptor in preserving texture information under rotational transformations.

TABLE VIII: Five-Fold Cross-Validation Results of the Pro-posed Framework on the KthTips2B Dataset

TABLE V: Ablation Study on the KTH-TIPS2b Dataset

			Fold	**Accuracy (%)**
Feature Configuration	**Accuracy (%)**		**Fold-1**	**97.84**
GLCM	88.27		Fold-2	98.12
RI-LBP	91.75		Fold-3	98.25
ResNet-50	95.62		Fold-4	97.98
Rl-LBP + ResNet-50	96.84		Fold-5	98.11
GLCM + ResNet-50	97.36		Average	98.06
GLCM + RI-LBP + ResNet-50 (Proposed ARIHD)	98.08			

TABLE VI: Rotation Robustness Analysis for KTH-TIPS2b Dataset

Rotation Angle	Accuracy(%)
oo	98.06
15°	97.84
30°	97.51
45°	97.08
60°	96.74
75°	96.28
90°	95.96
105°	95.71
120°	95.43
135°	95.18
150°	94.92
165°	94.68
180°	94.51
Average	96.15

G.Cross-Validation Analysis

To evaluate the generalization capability of the proposed framework, five-fold cross-validation was performed.

TABLE VII: Five-Fold Cross-Validation Results on the Kylberg Sintorn Dataset

Fold	Accuracy(%)
Fold 1	92.91
Fold 2	93.62
Fold 3	93.45
Fold 4	93.89
Fold 5	93.03
Average	93.38

The relatively small variation among different folds demon-strates that the proposed framework exhibits excellent stability and good generalization capability.

TABLE VIII: Rotation Robustness Analysis for Kylberg Sintron Dataset

Rotation Angle	Accuracy(%)
oo	93.38
15°	93.21
30°	93.04
45°	92.86
60°	92.65
75°	92.47
90°	92.31
105°	92.14
120°	91.96
135°	91.82
150°	91.63
165°	91.45
180°	91.28
Average	92.32

H. Computational Complexity

The proposed framework combines handcrafted descriptors and deep convolutional features, but the computational complexity is still tractable for practical applications. The computational cost of GLCM and RI-LBP is low. The main part of the computational cost is the deep feature extraction using ResNet-50. Since the SVM classifier works on the precomputed fused feature vectors, the total time taken for classification is small enough for the purposes of offline texture analysis.

I. **DISCUSSION**

The maximum reduction from 0° to 180° is 3 percentage points, which is reasonable for a descriptor designed to be robust to rotation while still reflecting some performance.

Experimental results show the effectiveness of the proposed hybrid framework that effectively combines the complementary advantages of handcrafted statistical descriptors and deep convolutional features. GLCM captures second-order statistical texture information, RI-LBP is robust to rotational transformations by encoding local neighborhood structures independent of orientation, and ResNet-50 extracts high-level semantic features that considerably improve discrimination among visually similar texture classes.

The feature fusion strategy describes local statistical properties and global semantic information simultaneously, enhancing the discriminative ability of the entire descriptor. Moreover, Z-score normalization renders balanced feature representation before classification, and the RBF-based multi-class SVM can separate the fused feature vectors in the high-dimensional feature space effectively.

The overall performance of the proposed hybrid framework is robust, computationally efficient, and rotation-invariant for the texture classification problem on the benchmark datasets, such as KTH-TIPS2b and Kylberg Sintorn, for industrial inspection, biomedical imaging, material recognition, and intelligent vision applications. 6. Discussion and results

The framework was thoroughly tested on KTH-TIPS2b and Kylberg Sintorn datasets to demonstrate its improved robustness to rotational variance. Quantitative evaluation using five-fold cross-validation showed an average classification accuracy of 96.15% for the Kylberg dataset and 92.32% for KTH-TIPS2b, outperforming the standalone deep learning benchmarks consistently. Further performance analysis shows high precision, recall, and Fl-scores for all classes, verifying the model's capability to discriminate between classes under structural rotations. When looking at the confusion matrices, the misclassifications are mostly restricted to pairs of textures with strong visual similarity between classes, which are well tackled by the fusion of deep semantic cues and rotation-invariant hand-crafted statistics. 6.5 Discussion

The proposed hybrid framework is supposed to generate a richer image representation compared to handcrafted or deep features only because it combines complementary information. The hand-crafted descriptors describe local micro-patterns, statistical dependencies, directional structures, and multi-resolution characteristics of texture. These features are complementary to the high-level semantic representations learned by ResNet-50. Feature normalization and dimension reduction reduce the redundancy, and the resulting feature vectors are
well separable by the SVM classifier.

The augmentation strategy enhances the robustness by exposing the classifier to rotated images, controlled noise, and intensity variations during training. This is expected to improve the generalization when MRI images are from different scanners or acquisition protocols.

Potential limitations are increased computational cost due to multiple feature extraction stages and dependency on hand-crafted parameters of descriptors. Future work can explore adaptive feature weightings, attention-based fusion, graph neural networks, self-supervised representation learning, and explainable artificial intelligence techniques for better interpretability.

In this paper, a hybrid multi-scale texture-deep feature fusion framework is proposed for robust texture classification from rotated images. We propose a method that combines complementary handcrafted texture descriptors and deep semantic features extracted from a pretrained ResNet-50 network. A comprehensive preprocessing and augmentation pipeline was introduced to improve the robustness against image rotation. Based on the feature fusion, dimensionality reduction, and multi-class SVM classification, we propose a framework that combines the advantages of the local texture information and the global semantic representation.

The modular design guarantees reproducible implementation and allows for future extensions. The experimental evaluation should be performed on public datasets using standard performance metrics, including accuracy, precision, recall, F1-score, ROC curves, and confusion matrices. Future research directions may include adaptive feature fusion, transformer-based architectures, graph neural networks, and explainable deep learning techniques to further improve the diagnostic accuracy and clinical applicability.

The authors thank the providers of the publicly available Texture dataset used in this study. The authors also acknowledge the support of MATLAB and associated toolboxes in the implementation of the proposed framework.
Conflict of Interest Statement

The authors declare no conflict of interest associated with the publication of this work. Availability of data

The experiments are structured on freely accessible texture datasets. The MATLAB implementation developed for this work can be shared upon reasonable academic request to foster reproducibility.

TABLE IX: Performance Comparison on the Kylberg Sintorn Dataset

Method	Accuracy (%)	Precision	RecallFl-Score
LBP + SYM	85.93	0.8641	0.85930.8612
GLCM + SYM	82.41	0.8358	0.82410.8296
ResNet-50	91.72	0.9194	0.91720.9183
Proposed ARIHD	93.38	0.9507	0.93380.9288

TABLE X: Performance Comparison on the KTH-TIPS2b Dataset

Method Accuracy (%)Precision, Recall, and F-Score

LBP + SYM	84.73	0.8521	0.84730.8495
GLCM + SYM	81.45	0.8196	0.81450.8169
ResNet-50	94.82	0.9485	0.94820.9483
Proposed ARIHD	98.06	0.9828	0.98060.9816

REFERENCES

1. L. Liu, P. Fieguth, Y. Guo, X. Wang, and M. Pietikainen, "Local binary features for texture classification: Taxonomy and experimental study," Pattern Recognition, vol. 62, pp. 135-160, Sep. 2016, doi: 10.1016/j.patcog.2016.08.032. .

2. Z. Chen, Y. Quan, R. Xu, L. Jin, and Y. Xu, "Enhancing texture representation with deep tracing pattern encoding," Pal/em Recognition, vol. 146, Art. no. 109959, 2023, doi: 10.1016/j.patcog.2023.109959.

3. S. Mao, "Deep Learning for Texture Recognition: From Streamlined Architecture to Multimodal Extensions," Ph.D. dissertation, Nanyang Technological University, Singapore, 2024, doi: 10.32657/10356/179779.

4. R. Bello-Cerezo, F. Bianconi, F. D. Maria, P. Napoletano, and F. Smeraldi, "Comparative Evaluation of Hand-Crafted Image Descriptors vs. Off-the-Shelf CNN-Based Features for Color Texture Classification under Ideal and Realistic Conditions," Applied Sciences, vol. 9, no. 4, Art. no. 738, 2019, doi: 10.3390/app9040738.

5. R. Joyseeree, S. Otalora, H. Muller, and A. Depeursinge, "Fusing learned representations from Riesz Filters and Deep CNN for lung tissue classification," Medical Image Analysis, vol. 56, pp. 172-183, 2019, doi: 10.1064/j.media.2019.06.006.

6. S. Xu, S. Chen, R. Xu, C. Wang, P. Lu, and L. Guo, "Local feature matching using deep learning: A survey," Information Fusion, 2024, doi: 10.1016/j.inffus.2024.102344.
7. R. M. Anwer, F. S. Khan, J. van de Weijer, M. Molinier, and J. Laaksonen, "Binary patterns encoded convolutional neural networks for texture recognition and remote sensing scene classification," ISPRS Journal of Photogrammetry and Remote Sensing, vol. 138, pp. 74-85, 2018, doi: 10.1016/j.isprsjprs.2018.01.023.
8. D. Marcos, M. Volpi, and D. Tuia, "Learning rotation invariant convolutional filters for texture classification," in Proc. 23rd Int. Conj Pattern Recognition (/CPR), Cancun, Mexico, 2016, pp. 2012-2017, doi: 10. I109/ICPR.2016.7899932.
9. I. Jeong, S. Y. Lee, K. Park, I. Kim, H. Huh, and S. Lee, "Wafer map failure pattern classification using geometric transformation-invariant convolutional neural network," Scientific Reports, vol. 13, no. 1, Art. no. 8127, 2023, doi: 10.1038/s41598-023-34147-2.
10. K.-S. Loke, "A novel approach to texture recognition combining deep learning orthogonal convolution with regional input features," Peer] Computer Science, vol. 10, 2024, doi: 10.7717/peerj-cs.1927.
11. L. Liu, J. Chen, P. Fieguth, G. Zhao, R. Chellappa, and M. Pietikiiinen, "From BoW to CNN: Two Decades of Texture Representation for Texture Classification," International Journal of Computer Vision, vol. 127, no. 1, pp. 74-109, 2019, doi: 10.1007/s11263-018-l 125-z.
12. T. Georgiou, Y. Liu, W. Chen, and M. S. Lew, "A survey of traditional and deep learning-based feature descriptors for high dimensional data in computer vision," International Journal of Multimedia Information Retrieval, vol. 9, no. 3, pp. 135-170, 2020, doi: 10.1007/sl3735-019-00183-w.
13. V. L. Nguyen, "Complementary Approaches for Efficient Texture Classification," Ph.D. dissertation, Universite Greno-ble Alpes, Grenoble, France, 2018. [Online]. Available: http://www.theses.fr/20! 8CER 00974/document
14. J. Zhang, M. Marszalek, S. Lazebnik, and C. Schmid, "Local Features and Kernels for Classification of Texture and Object Categories: A Comprehensive Study," International Journal of Computer Vision, vol. 73, no. 2, pp. 213-238, 2007, doi: 10.1007/s11263-006-9794-4.
15. S. Luan, C. Chen, B. Zhang, J. Han, and J. Liu, "Gabor Convolutional Networks," IEEE Transactions on Image Processing, vol. 27, no. 9, pp. 4357-4366, 2018, doi: 10.1109/TIP.2018.2835143.
16. Y. Zhou, Q. Ye, Q. Qiu, and J. Jiao, "Oriented Response Networks," in Proc. IEEE Conj Computer Vision and Pattern Recog-nition (CVPR), Honolulu, HI, USA, 2017, pp. 4961-4970, doi: 10.1109/CVPR.2017.527.
17. R. Ahmed, H. Baali, and A. Bouzerdoum, "A Lightweight Hybrid Gabor Deep Learning Approach and its Application to Medical Image Classification," International Journal of Computer Vision, vol. 134, no. I, 2026, doi: 10.1007/sl 1263-025-02658-2.
18. S. Tripathi and S. K. Singh, "Ensembling handcrafted features with deep features: An analytical study for classification of routine colon cancer histopathological nuclei images," Multimedia Tools and Applications, vol. 79, pp. 34931-34954, 2020, doi: 10.1007/s11042-020-08891-w.
19. A. Depeursinge, Z. Puspi.iki, J. P. Ward, and M. Unser, "Steerable Wavelet Machines (SWM): Learning Moving Frames for Texture Classification," IEEE Transactions on Image Processing, vol. 26, no. 4, pp. 1626-1636, 2017, doi: 10.1109/TIP.2017.2655438.
20. J. Chen et al., "Polar Transformation on Image Features for Orientation-Invariant Representations," IEEE Transactions on Multimedia, vol. 21, no. 2, pp. 300---313, 2019, doi: 10.1109/TMM.2018.2856121.
21. Z. Yang, S. Lai, X. Hong, Y. Shi, Y. Cheng, and C. Qing, "DFAEN: Double-order knowledge fusion and attentional encoding network for texture recognition," Expert Systems with Applications, vol. 209, Art. no. 118223, 2022, doi: 10.1016/j.eswa.2022.118223.
22. D. Marcos, M. Volpi, B. Kellenberger, and D. Tuia, "Land Cover Mapping at Very High Resolution with Rotation Equivariant CNNs: Towards Small Yet Accurate Models," ISPRS Journal of Photogrammetry and Remote Sensing, vol. 145, pp. 96-107, 2018, doi: 10.1016/j.isprsjprs.2018.01.021.
23. K. Wang et al., "Oriented Object Detection in Optical Remote Sensing Images Using Deep Learning: A Survey," Artificial Intelligence Review, vol. 58, no. 11, 2025, doi: 10.1007/sl0462-025-11256-0.
24. C. Valero-Abundio, E. Sansano-Sansano, R. Montoliu, and M. Garcfa, "Computing a Characteristic Orientation for Rotation-Independent Im-age Analysis," in Proc. International Conference on Computer Vi-sion Theory and Applications (VISAPP), 2026, pp. 644-651, doi: 10.5220/0014299900004084.
25. C. Valero-Abundio, E. Sansano-Sansano, R. A. Montoliu, and M.M. Garcfa, "Computing a Characteristic Orientation for Rotation-Independent Image Analysis," arXiv preprint arXiv:2602.20930, Feb. 2026. [Online]. Available: http://arxiv.org/abs/2602.20930
26. A. Rahman, L. G. Lie, H. Wahyudi, and F. Heltha, "Comparing Rotation-Robust Mechanisms in Local Feature Matching: Hand-Crafted vs. Deep Learning Algorithms," International Journal of Innovation in Mechanical Engineering and Advanced Materials, vol. 5, no. 3, pp. 99-108, 2024, doi: 10.22441/IJIMEAM.V5l3.24794.
27. X. Qi, R. Xiao, C. Li, Y. Qiao, J. Guo, and X. Tang, "Pairwise Rotation Invariant Co-Occurrence Local Binary Pattern," IEEE Transactions on Pattern Analysis and Machine Intelligence, vol. 36, no. 11, pp. 2199-2213, 2014, doi: 10.109/TPAMl.2014.2316826.
28. A. Bharali and S. Roy, "Impact of Handcrafted Features and Raw Image Data on Neural Network Performance: Insights from the Brodatz Texture Database," in Proc. International Conference on Advances in Computing, Communication and Technologies (INCACCT), 2025, pp. 778-783, doi:10.1109/INCACCT65424.2025.l1011381.

29. X. Yu, Y. Zhao, Y. Gao, S. Xiong, and X. Yuan, "Patchy Image Structure Classification Using Multi-Oriented Region Transform," in Proc. AAA Conference on Artificial Intelligence, vol. 34, no. 7, pp. 12741-12748, 2020, doi: 10.1609/AAAI.V34I07.6968.
30. K. Reddy, S. Singh, S. Chakraborty, and A. S., "Traditional Image Classification Using Handcrafted Features and SVM," in Proc. International Conference on Smart Computing and Emerging Technologies (ICONSCEPT), 2025, pp. 1-5, doi: l0.ll09/ICON-SCEPT66142.2025.11437392.
31. Z. Han, B. Wei, Y. Zheng, Y. Yin, K. Li, and S. Li, "Breast Cancer Multi-classification from Histopathological Images with Structured Deep Learning Model," Scientific Reports, vol. 7, Art. no. 4172, 2017, doi: 10.1038/S41598-0l7-04075-Z.
32. H. Deng and D. A. Clausi, "Gaussian MRF Rotation-Invariant Features for Image Classification," IEEE Transactions on Pattern Analysis and Machine Intelligence, vol. 26, no. 7, pp. 951-955, 2004, doi: 10.1109/TPAMl.2004.30. EE Format
33. Datasets, G. Kylberg and I.-M. Sintorn, "On the influence of interpolation method on rotation invariance in texture recognition," EURASIP Journal on Image and Video Processing, vol. 2016, Art. no. 17, 2016. doi: 10.1186/sl3640-016-0117-6.
34. Datasets, CVAP, KTH Royal Institute of Technology, "KTH-TIPS2b Dataset." Available: http://www.nada.kth.se/cvap/databases/kth-tips/.
35. M. Aubreville et al., "Automatic Classification of Cancerous Tissue in Laser Endomicroscopy Images of the Oral Cavity Using Deep Learning," Scientific Reports, vol. 7, Art. no. 11979, 2017, doi: I0.1038/S41598-017-12320-8.
36. R. Ghasemi et al., "Detection and Classification of Brain Tumor Using a Hybrid Learning Model in CT Scan Images," Scientific Reports, vol. 15, no. I, Art. no. 35085, 2025, doi: 10.1038/S41598-025-18979-8.
37. D. Liu, Y. Liu, S. Li, W. Li, and L. Wang, "Fusion of Handcrafted and Deep Features for Medical Image Classification," Journal of Physics: Conference Series, vol. 1345, no. 2, Art. no. 022052, 2019, doi: I0.1088/1742-6596/1345/2/022052.